Chitosan-Catalyzed Aggregation during the Biomimetic Synthesis of Silica Nanoparticles

Jenq-Sheng Chang, Zwe-Ling Kong, Deng-Fwu Hwang, and Ke Liang B. Chang*

Department of Food Science, National Taiwan Ocean University, 2 Pei-Ning Road, Keelung 20224, Taiwan

Received September 27, 2005. Revised Manuscript Received November 22, 2005

Silicate is polymerized in the presence of chitosan to form novel silica−chitosan nanoparticles in weakly acidic solution under ambient conditions. Both the turbidity of the silica solution and the average hydrodynamic diameter of the silica nanoparticles increased dramatically after the addition of chitosan. The initial stage of silica formation closely observed fourth-order kinetics. The latter transformation of colloidal nanoparticles approximated an exponential growth pattern during slow aggregation. Chitosan did not significantly change the rate of silica synthesis and the size of the individual nanoparticles, but it facilitated an aggregation of the composite nanoparticles by 1 order of magnitude faster than for pure silica nanoparticles. Scanning electron microscopy revealed that the composite nanoparticles grew in three dimensions and became clusters and aggregates within a shorter time. Atomic force microscopy demonstrated that the composite nanoparticles increased from as small as 1 nm to 32 nm after a reaction time of 1 and 24 h, respectively. X-ray diffraction, infrared spectroscopy, and elemental analysis confirmed that these nanoparticles were amorphous composites of silica and chitosan. Synthesis of silica with chitosan provided a facile way of preparing composite silica nanoparticles with improved functional properties.

Introduction

Nature abounds with examples of integrating organic and inorganic compounds to form biological structures. Nanocomposite materials of polymer and silica have attracted much interest in recent years because they often encompass the desirable features of both organic and inorganic compounds. Those materials consisting of silica are also attractive from both economic and scientific perspectives because silicon is the second most abundant element in the Earth's crust.

Silica nanostructures allow one to encapsulate biomolecules,[1] produce sensing and imaging nanoparticles for biotechnology,[2] and deliver multiple clinical functions.[3] Most prior research used the sol−gel process to create mesoporous material, silica nanoparticles, and nanostructures. For instance, Kresege and co-workers[4] described the synthesis of molecular sieves by templating with liquid crystals. Many other researchers have used surfactants to form the templates for preparing mesoporous materials.[5] Wei et al.[6] reported that nonsurfactant compounds could also template the formation of mesoporous silica. Although harsh conditions (e.g., the use of an acid catalyst and the formation of methanol or ethanol) are usually encountered during sol−gel synthesis, silica has been made into nanotubes functionalized with silane, antibodies, or enzymes,[7] as well as bioactive xerogels for controlled-release applications.[8]

Silica is present in diatom skeletons, sponge spicules, plant phytoliths, and animal dietary silicon. Its natural and exquisite structures have inspired a myriad of biomimetic syntheses of silica nanomaterials.[9−12] Polypeptides, silaffin,[13] and polyamines[14,15] extracted from diatoms can regulate biosilica morphogenesis under mild conditions. Another polypeptide, silicatein,[16] which is extracted from sponges, exhibits comparable capabilities. Natural and synthetic analogues of silaffin and silicatein, as well as lysozyme,[17] block copolypeptides,[18] poly-L-lysine/poly(allylamine hydrochloride),[19] and small molecules,[20] will also catalyze silica

* To whom correspondence should be addressed. Tel.: 886-2-24622192, ext. 5125. Fax: 886-2-24634203. E-mail: klchang@mail.ntou.edu.tw.

(1) Gill, I.; Ballesteros, A. *Trends Biotechnol.* **2000**, *18*, 282−296.
(2) Tan, W.; Wang, K.; He, X.; Zhao, X. J.; Drake, T.; Wang, L.; Bagwe, R. P. *Med. Res. Rev.* **2004**, *24*, 621−638.
(3) Levy, L.; Sahoo, Y.; Kim, K. S.; Bergey, E. J.; Prasad, P. N. *Chem. Mater.* **2002**, *14*, 3715−3721.
(4) Kresege, C. T.; Leonowicz, M. E.; Roth, W. J.; Vartuli, J. C.; Beck, J. S. *Nature* **1992**, *359*, 710−713.
(5) Lin, H. P.; Mou, C. Y. *Acc. Chem. Res.* **2002**, *35*, 927−935.
(6) Wei, Y.; Xu, J.; Dong, H.; Dong, J.; Qiu, K.; Jansen-Varnum, S. A. *Chem. Mater.* **1999**, *11*, 2023−2029.
(7) Mitchell, D. T.; Lee, S. B.; Trofin, L.; Li, N.; Nevanen, T. K.; Söderlund, H.; Martin, C. R. *J. Am. Chem. Soc.* **2002**, *124*, 11864−11865.
(8) Radin, S.; El-Bassyouni, G.; Vresilovic, E. J.; Schepers, E.; Ducheyne, P. *Biomaterials* **2005**, *26*, 1043−1052.
(9) Zaremba, C.; Stuckyt, G. D. *Science* **1996**, *1*, 425−429.
(10) Morse, D. E. *Trends Biotechnol.* **1999**, *17*, 230−232.
(11) Perry, C. C.; Keeling-Tucker, T. *J. Biol. Inorg. Chem.* **2000**, *5*, 537−550.
(12) Coradin, T.; Lopez, P. J. *ChemBioChem* **2003**, *4*, 251−259.
(13) Kröger, N.; Deutzmann, R.; Sumper, M. *Science* **1999**, *286*, 1129−1132.
(14) Kröger, N.; Deutzmann, R.; Bergsdorf, C.; Sumper, M. *Proc. Natl. Acad. Sci. U.S.A.* **2000**, *97*, 14133−14138.
(15) Kröger, N.; Lorenz, S.; Brunner, E.; Sumper, M. *Science* **2002**, *298*, 584−586.
(16) Shimizu, K.; Cha, J.; Stucky, G. D.; Morse, D. E. *Proc. Natl. Acad. Sci. U.S.A.* **1998**, *95*, 6234−6238.
(17) Coradin, T.; Coupé, A.; Livage, J. *Colloid Surf., B* **2003**, *29*, 189−196.
(18) Cha, J. N.; Stucky, G. D.; Morse, D. E.; Deming, T. J. *Nature* **2000**, *403*, 289−292.
(19) Patwardhan, S. V.; Clarson, S. J. *J. Inorg. Organomet. Polym.* **2002**, *12*, 109−112.
(20) Coradin, T.; Livage, J. *Colloid Surf., B* **2001**, *21*, 329−336.

10.1021/cm052161d CCC: $33.50
Published on Web 12/31/2005

synthesis at near-neutral pH. Even polysaccharides such as alginate,[21] carageenan,[21] and cationic hydroxyethylcellulose[21,22] promoted silica formation from tetrakis (2-hydroxyethyl) orthosilicate during the sol−gel process. This excellent prior work demonstrates that the biomimetic synthesis of silica has been in practice for years, yet the kinetics of biosilicification remains largely unexplored. In fact, biomimetics has been more an art than a science.

Chitin, poly-β-(1,4)-2-acetamido-2-deoxy-D-glucopyranose, is the second most abundant carbohydrate on earth. It is the structural polysaccharide present in the shells of crustaceans, in the cell walls of fungi and yeasts, and in squid pens.[23] After deacetylation by hot alkali, chitin becomes chitosan, a polymer with varying proportions of *N*-acetylglucosamine and glucosamine repeating units. Chitosan has many potential applications in various industries.[24,25] For instance, silica and chitosan composites have been prepared and used to improve the integrity and dimensional stability of aerogels.[26] Recently, chitosan was found to perform well when used in coated silica beads[27] as a chromatography sorbent or as a composite membrane[28] for tissue-engineering applications. However, the kinetics of reactions involving chitosan in the preparation of silica nanoparticles under conditions close to those of biosilicification processes has never been explored.

In this study, we combined several physicochemical techniques to examine how a cationic polysaccharide, chitosan, affected the kinetics of silica synthesis. This report presents an in-depth analysis of the biomimetic synthesis of silica nanoparticles from chitosan and sodium silicate under weakly acidic conditions at room temperature. The kinetic behavior of silica polymerization and the growth patterns of nanoparticles help provide a better picture of how biopolymers may assist in silica formation in nature.

Experimental Section

Preparation of Silica Nanoparticles. Chitosan samples purchased from a commercial supplier (Lytone Enterprise, Inc., Taipei, Taiwan) were analyzed for the degree of deacetylation (DD) and molecular weight (MW) according to previous reports.[29] More specifically, chitosan was dissolved in 1% acetic acid to form a 0.1% (w/v) solution. Size-exclusion chromatography (SEC) was performed by using 10 pullulan standards with molecular weights between 1300 and 788 000 Da. Each 20 μL aliquot of chitosan was filtered through a 0.45 μm syringe filter and injected into the HPSEC using TSK G4000PW(XL) and TSK PW6000PW(XL) (Tosoh) GFC columns in series. The remaining SEC details were as described in our previous report.[29] The DDs of the chitosan samples were 76, 81, 86, and 90%, with corresponding MWs of 500, 200, 70, and 20 kDa, respectively. Sodium silicate was dissolved in a 0.05 M sodium acetate solution (which was adjusted to different pH levels with different amounts of acetic acid) to prepare a 0.82% (w/w) sodium silicate solution. After agitating 30 mL of a sodium silicate solution for 10 min using a magnetic stirrer, we added 3 mL of a chitosan solution (0.28% w/w). The resulting solution, containing silicate (0.04641 M) and chitosan (0.000509−0.0127 mM), was mixed completely. Afterward, it was moved from the stirrer to the benchtop. The solution was left undisturbed and periodically monitored for the change in the concentration of silicic acid and small silica oligomers,[30] turbidity, and particle size. The molybdosilicate titration method described in a previous report[30] was used to determine the concentration of silicic acid and small silica oligomers by comparing with the standardization curve established with different concentrations of a sodium silicate solution.

Analytical. Laser light-scattering photon-correlation spectroscopy was performed at 25 °C (90° angle) to measure the size of the nanoparticles with a Malvern 4700c submicron particle analyzer (Malvern Instruments, Malvern, Worcestershire, U.K.) equipped with a helium neon laser with a wavelength output of 633 nm. Silica or silica−chitosan nanoparticles were suspended in 15 mL of deionized water. Each 2 mL sample was placed in a quartz tube and measured for the time-averaged particle diameter. The particle-size data were collected over an analysis time of at least 5 min. A Hitachi S-4100 scanning electron microscope (SEM) and an NTMDT P47H atomic force microscope (AFM) were used to observe the change in particle size and morphology of nanoparticles after their formation and aggregation. Freeze-dried nanoparticles were distributed on top of the glass. A layer of gold was deposited, and the micrographs were taken at 20 kV in the SEM. For atomic force microscopy, a silicon wafer was rinsed thoroughly with alcohol. The nanoparticle solution was dripped onto the wafer. After standing for 10 min, the wafer was dried and observed in the AFM. X-ray diffraction (XRD) was used to examine the structure of the silica nanoparticles. Diffraction data were recorded using a Siemens D-5000 X-ray diffractometer with Cu Kα radiation (λ = 1.54051 Å) in the scanning mode from 10 to 80° 2θ in steps of 0.05° with a collection time of 1 s per step. Fourier transform infrared spectroscopy (FTIR) was used to analyze the molecular structure of silica nanoparticles. Tablets were made of freeze-dried silica nanoparticles and potassium bromide at a ratio of 1:100 (w/w). The IR absorbance was determined with a Bio-Rad FTS-155 infrared spectrometer. Elemental analysis was performed on a Heraeus Vario EL-III CHN analyzer using acetanilide as the standard. For the determination of the carbon, hydrogen, and nitrogen content, the accuracy of the instrument was ±0.1% and the precision was ±0.2%

Results and Discussion

Kinetics of Silica Synthesis. Before the concentration of silicic acid and soluble silica oligomers decreases beyond detectability, the polymerization of silica occurs with a reaction rate that has usually been reported with a reaction order of 1−5.[31] The polymerization is generally believed to start with the condensation of two monosilicic acid molecules

$$Si(OH)_4 + Si(OH)_4 \rightarrow (HO)_3Si\text{-}O\text{-}Si(OH)_3 + H_2O \quad (1)$$

Further polymerization steps lead to the formation of trimers,

(21) Shchipunov, Yu. A.; Karpenko, T. Yu. *Langmuir* **2004**, *20*, 3882−3887.
(22) Shchipunov, Yu. A.; Kojima, A.; Imae, T. *J. Colloid Interface Sci.* **2005**, *285*, 574−580.
(23) Knorr, D. *Food Technol.* **1984**, *38* (1), 85−97.
(24) Muzzarelli, R. A. A. *Carbohydr. Polym.* **1983**, *3*, 53−75.
(25) Ravi Kumar, M. N. V. *React. Funct. Polym.* **2000**, *46*, 1−27.
(26) Ayers, M. R.; Hunt, A. J. *J. Non-Cryst. Solids* **2001**, *285*, 123−127.
(27) Rashidova, S. S.; Shakarova, D. S.; Ruzimuradov, O. N.; Satubaldieva, D. T.; Zalyalieva, S. V.; Shpigun, O. A.; Varlamov, V. P.; Kabulov, B. D. *J. Chromatogr., B* **2004**, *800*, 49−53.
(28) Suzuki, T.; Mizushima, Y.; Umeda, T.; Ohashi, R. *J. Biosci. Bioeng.* **1999**, *88*, 194−199.
(29) Chang, K. L. B.; Tai, M. C.; Cheng, F. H. *J. Agric. Food Chem.* **2001**, *49*, 4845−4851.
(30) Coradin, T.; Durupthy, O.; Livage, J. *Langmuir* **2002**, *18*, 2331−2336.
(31) Perry, C. C.; Keeling-Tucker, T. *J. Biol. Inorg. Chem.* **2000**, *5*, 537−550.

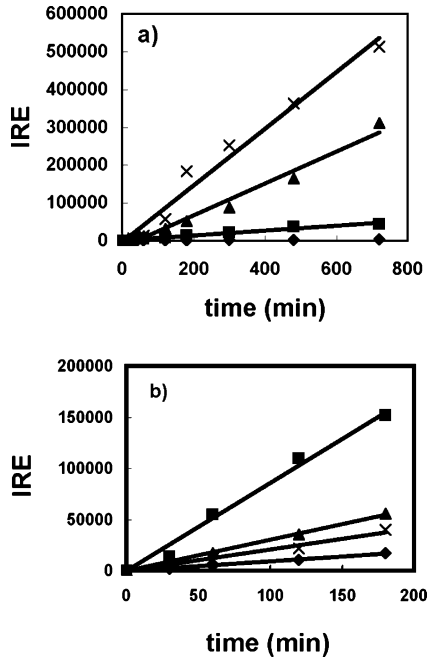

Figure 1. Fourth-order reaction of silica polycondensation (a) at different pH values (labels: diamond, pH 4; square, pH 4.6; triangle, pH 5; cross, pH 5.6) and (b) at pH 5.6 after the addition of chitosan with different molecular weights (labels: diamond, $M_w = 500$ kDa; square, $M_w = 200$ kDa; triangle, $M_w = 70$ kDa; cross, $M_w = 20$ kDa).

tetramers, pentamers, and so on. In contrast to the polymerization of organic molecules, the condensation of silica does not need to proceed in a linear fashion. The oligomers may grow three-dimensionally and become colloidal silica spheres or create a gel network. The colorimetric method,[30,32] based on the absorption measurement of a yellow silicomolybdic acid solution, was found to indicate the total concentration (soluble Si-containing compounds, SSC) of silicic acid and soluble silica oligomers with $n \leq 4$. As a consequence, one would expect the change in SSC concentration to observe second-, third-, or fourth-order kinetics. The reaction rate equation for an *n*th-order reaction is as follows

$$r = -\mathrm{d[C]}/\mathrm{d}t = k_n[\mathrm{C}]^n \qquad (2)$$

When $n = 4$, the integration of the above equation yields the integrated rate equation[33] (IRE)

$$k_4 t = \frac{1}{3}\left[\left(\frac{1}{C}\right)^3 - \left(\frac{1}{C_0}\right)^3\right] \equiv \mathrm{IRE} \qquad (3)$$

In the above equations, k is the rate constant in $\mathrm{M}^{-3}\ \mathrm{min}^{-1}$ or $\mathrm{mM}^{-3}\ \mathrm{s}^{-1}$, t represents the reaction time in min or s, and C stands for the concentration of SSC in M (C_0, the initial concentration). Consequently, a plot of the IRE (M^{-3}) as a function of time would be linear, and the slope of the regression line is k_4. Figure 1a shows that the decrease in SSC during the initial stage of the reaction obeyed fourth-order kinetics closely. The rate constant increased with increasing pH in acidic solutions. It changed from 1.11×10^{-10} to 1.12×10^{-9}, 6.43×10^{-9}, and $1.24 \times 10^{-8}\ \mathrm{mM}^{-3}\ \mathrm{s}^{-1}$ when the pH was raised from 4 to 4.6, 5, and 5.6, respectively. These results were in good agreement with the observations in a recent report[33] for silica synthesis in a dilute aqueous solution. A further increase in pH to 6 and above resulted in a reaction so rapid that it deviated from the linear behavior in a short time.

Effect of Chitosan on Silica Synthesis. When we added chitosan to the solution, the reaction order for the initial stage of the silica synthesis remained the same (Figure 1b). A test of the kinetic data (see the Supporting Information) as an *n*th-order reaction suggested that the polymerization of silica in the presence of chitosan conformed more closely to a two-stage process with a reaction order of n, where $n = 1$, 2, 3, or 5. The two stages of the reaction bordered at ca. 120 min after the addition of chitosan. These results helped explain why there have been so many contradictions among literature reports, in which the kinetics of silica condensation has been reported to range from first- to fifth-order.[31,33,34] Nevertheless, the fourth-order kinetics provided a relatively good agreement between a single regression line and experimental data. This result was similar to our data for a pure silica synthesis and those shown for silica oligomerization in a recent report.[33]

The rates of silica polymerization were influenced by both the presence of chitosan and the MW of chitosan (Figure 1b). The largest rate constant ($1.44 \times 10^{-8}\ \mathrm{mM}^{-3}\ \mathrm{s}^{-1}$) occurred at a MW of 200 kDa, followed by lower values of 5.07×10^{-9}, 3.47×10^{-9}, and $1.56 \times 10^{-9}\ \mathrm{mM}^{-3}\ \mathrm{s}^{-1}$ at 70, 20, and 500 kDa, respectively. A further decrease in MW produced samples with no apparent change in the reactant consumption rate. Chitosan with a molecular weight of 500 kDa had the smallest number of amino groups, the lowest solubility, and the highest viscosity in the test solution. This may make it less likely to interact with SSC molecules and lead to the lowest rate constant among all samples. With the exception of the 200 kDa chitosan, the rate constants after the addition of chitosan at pH 5.6 became slightly smaller than that obtained for pure silica formation at the same pH ($1.24 \times 10^{-8}\ \mathrm{mM}^{-3}\ \mathrm{s}^{-1}$). This might be due to the fact that the initial concentration of SSC dropped from 0.04641 to 0.0222−0.0311 M upon the addition of chitosan. We speculate that the positively charged amino groups in chitosan attracted SSC from the solution. This would make them become insoluble and nondetectable by the colorimetric method of the solution. Further reduction in SSC was therefore slower, as the reaction shifted from a lower chemical potential toward the equilibrium state between the SSC and insoluble silica.

Change in the Turbidity of the Solution. The silica solution was transparent at first, and it underwent polycondensation slowly under ambient conditions. After a certain reaction time, the solution became opaque as a result of silica nanoparticles aggregating and significantly increasing in size. As a consequence, the turbidity of the silica solutions (see the Supporting Information) increased slowly over 3600 min to 95 NTU (nephelometric turbidity units). The rate of increase became significantly higher afterward, and the

(32) Tanaka, M.; Takahashib, K. *Anal. Chim. Acta* **2001**, *429*, 117−664.
(33) Icopini, G. A.; Brantley, S. L.; Heaney, P. J. *Geochim. Cosmochim. Acta* **2005**, *69*, 293−303.
(34) Perry, C. C.; Keeling-Tucker, T. *Colloid Polym. Sci.* **2003**, *281*, 652−664.

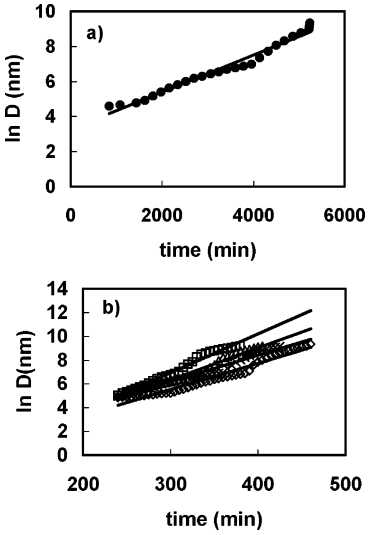

Figure 2. Time-resolved size analysis of (a) silica nanoparticles and (b) silica−chitosan (labels: diamond, $M_w = 500$ kDa; square, $M_w = 200$ kDa; triangle, $M_w = 70$ kDa; cross, $M_w = 20$ kDa) nanoparticles in solution.

turbidity reached 1000 NTU at ca. 5230 min. When chitosan was added to the silica solution, the turbidity increased much more rapidly. It reached 1000 NTU within 318−400 min, depending on the MW of the chitosan. Because the change in turbidity was related to the aggregation of silica nanoparticles, these observations suggested that silica nanoparticles aggregated ca. 1 order of magnitude faster upon the addition of chitosan.

Kinetics of Nanoparticle Aggregation. The addition of chitosan not only increased the rate of turbidity change but also increased the rate of nanoparticle size enlargement. Figure 2 shows the particle size of silica nanoparticles from the light-scattering measurement. Because of the transparency of small nanoparticles, we were unable to obtain stable signals when they were below ca. 50 nm. At pH 5.6, the silica nanoparticle in the silicate solution was ca. 98 nm after 840 min. It enlarged to ca. 1000 nm after a reaction time of 3780−3960 min. When chitosan was added to the silicate solution, the nanoparticles grew rapidly in size. The silica nanoparticles grew to 1000 nm in 300 min in the presence of 200 kDa chitosan. In comparison, the time to grow to 1000 nm was 390, 340, and 360 min when the MW of the chitosan was 500, 70, and 20 kDa, respectively. The kinetic equation for the slow aggregation of colloidal silica was reported to conform to the exponential growth equation,[35] $M_w \approx e^{kt}$. If we assume the silica particles have a uniform density, then their molecular weights would be proportional to their sizes ($\sim D^3$). Consequently, the exponential growth of the silica cluster size could be related to the reaction time by

$$D = 2R = D_0 e^{k't} \tag{4}$$

$$\ln D = \ln D_0 + k't \tag{5}$$

In the above equation, t is time, D is the growth of the average aggregated cluster diameter, and k' represents the rate constant of the slow aggregation stage. The slope of the graph in Figure 2a, which represents the rate constant k' for silica aggregation without chitosan, has a value of 0.0011 nm/min. The effect of chitosan with different MWs on the growth of the silica nanoparticle was similar to its effect on the increase in turbidity. In the presence of chitosan (Figure 2b), k' became approximately 0.0221, 0.0326, 0.0267, and 0.022 nm/min when chitosan with MWs of 500, 200, 70, and 20 kDa, respectively, was added to the solution. In other words, the aggregation rate constant increased ca. 20−30-fold upon the addition of chitosan. Because of the significant increase in the aggregation rate and the size of nanoparticles, the kinetic data deviated slightly from a single regression line after a shorter reaction time. This suggested that two-stage kinetics similar to that described in a recent report[36] might evolve during silica nanoparticle aggregation. The simplicity of the initial one-stage slow-aggregation rate equation, however, could provide a convenient tool for analyzing the size evolution of silica nanoparticles in the presence of catalytic molecules such as chitosan and other biomolecules such as polypeptide, silaffin, or silicatein. Although aggregation is undesirable for products that are to be used in the solution, the aggregation of silica−chitosan composite nanoparticles makes them settle in the centrifuge more readily within a shorter time than that for pure silica nanoparticles. These characteristics may help make the preparation of these composite nanoparticles more economical for chromatographic or analytical applications.

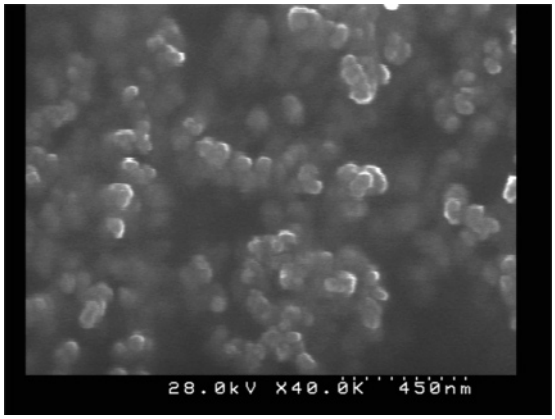

Figure 3. SEM image of freeze-dried silica−chitosan nanoparticles formed 24 h after the addition of chitosan to the sodium silicate solution (0.04641 M sodium silicate + 0.001273 M chitosan with a molecular weight of 200 kDa).

Size Evolution of Silica Nanoparticles. Electron microscopy confirmed that the increase in nanoparticle size did originate from the aggregation of smaller nanoparticles. The scanning electron micrographs (Figure 3) show that the freeze-dried silica−chitosan nanoparticles consist of clusters of nanoparticles much smaller than 100 nm. The AFM micrographs reveal that diluted silica−chitosan nanoparticles had an average size of 1.2 nm after a reaction time of 1 h, 8.6 nm after 4 h, and ca. 32 nm after 24 h (Figure 4). As a comparison, the light-scattering measurement recorded an average size of ca. 154 nm at 240 min and grew to 9.7 μm 380 min after the addition of chitosan. Consequently, the

(35) Martin, J. E.; Wilcoxon, J. P.; Schaefer, D.; Odinek, J. *Phys. Rev. A* **1990**, *41*, 4379−4391.

(36) Huang, F.; Zhang, H.; Banfield, J. F. *Nano Lett.* **2003**, *3*, 373−378.

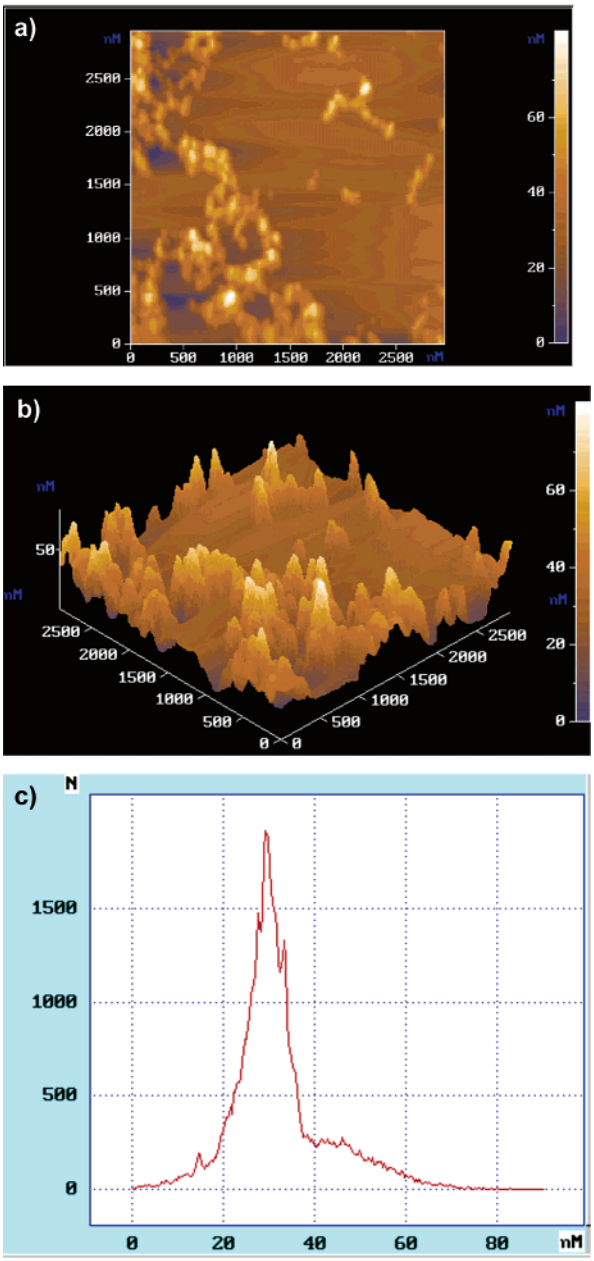

Figure 4. AFM images (a, b) and particle size distribution (c) of silica−chitosan nanoparticle structures formed 24 h after the addition of chitosan to the sodium silicate solution (0.04641 M sodium silicate + 0.001273 M chitosan with a molecular weight of 200 kDa).

light-scattering data (Figure 2) imply that the silica nanoparticles aggregated to form clusters with large average apparent diameters in the solution. By combining the reactant concentration, turbidity, light-scattering, and electron microscope data, we can propose the following mechanism for silica synthesis in the presence of chitosan. For a linear cationic polysaccharide such as chitosan, it may attract silicic acid in the solution through ionic interaction with its protonated amino groups, H_3N^+, on C2 or through hydrogen bonding with the hydroxyl groups on C3 and C6. These attracted molecules subsequently provide a template for further silica synthesis. Furthermore, these intermolecular interactions help to shorten the distance for silica to contact other growing silica particles during the polycondensation of oligomers. They facilitate the aggregation of silica nanoparticles in two dimensions, appearing as a pearl

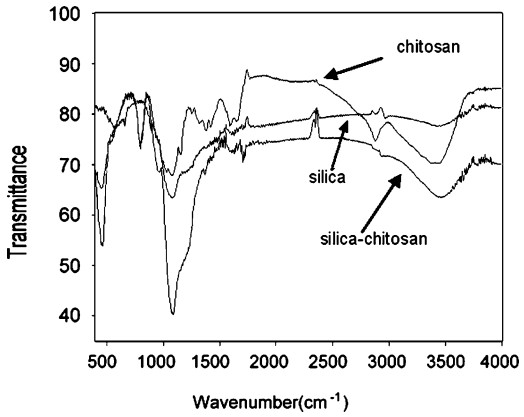

Figure 5. FTIR spectra of chitosan, silica nanoparticles, and silica−chitosan nanoparticles.

Table 1. Approximate Composition Calculated from the Elemental Analysis Data

sample	Si (%)	O (%)	N (%)	C (%)	H (%)
chitosan		46.54	7.315[a]	38.91[a]	7.235[a]
silica nanoparticle	45.5[b]	51.9[b]		0.76[a]	1.8[a]
silica−chitosan nanoparticle	39.8[c]	49.2[c]	0.75[a]	7.1[a]	3.2[a]

[a] Average of duplicate measurements of elemental analysis. [b] Calculated by assuming the silicon-to-oxygen ratio is the same as that in SiO_2 (46.7:53.25). [c] Calculated by accounting for the oxygen content of both chitosan and silica in composite nanoparticles.

necklace, or even in three dimensions, appearing as a bunch of grapes. As a consequence, the aggregation rate increased significantly, even though silica tends to form small nanoparticles in acidic solution.[31]

Structural Characteristics of Composite Nanoparticles. Figure 5 shows the FTIR spectra for silica, chitosan, and silica−chitosan nanoparticles. The wavenumbers at 460, 790, 950, 1090, 1640, and 3440 cm^{-1} represent the bonds of Si−O, Si−O−Si, Si−O−N, and OH^-, respectively. In the absorption spectrum of chitosan, amide groups appeared at 1655 and 1550 cm^{-1}. The absorption peaks characteristic of both silica and chitosan appeared in the silica−chitosan nanoparticle spectrum. Furthermore, an additional peak at 950 cm^{-1} was observed. This corresponds to Si−OH bond stretching. These results were similar to those reported in the literature[37] for the IR spectrum of silica.

X-ray diffraction (see the Supporting Information) shows a broad signal at $2\theta = 23°$, indicating that the silica nanoparticles were amorphous. The silica−chitosan nanoparticles had a scattered intensity stronger than that of the silica nanoparticles. Repeat runs with exactly the same weight of nanoparticles result in similar patterns. Although the real cause for this phenomenon requires further investigation, it might imply that silica−chitosan nanoparticles were more closely packed. Elemental analysis (Table 1) revealed that silica−chitosan nanoparticles contained approximately 10% chitosan. This ratio was close to the weight ratio of chitosan and silicic acid in the reaction medium. The silicon content of the silica nanoparticles was ca. 46% due to the presence of a small amount of carbon (0.8%) and hydrogen (1.8%). The silicon content of the silica−chitosan nanoparticles was lowered to 40% as a result of the addition of chitosan. These

(37) Benning, L. G.; Phoenix, V.; Yee, N.; Tobin, M. J. *Geochim. Cosmochim. Acta* **2004**, *68*, 729−741.

data provided quantitative evidence that silica formed a composite nanomaterial with chitosan in the particles.

Conclusion

In conclusion, we have demonstrated that chitosan, an aminoglycan, could catalyze the slow aggregation of colloidal silica nanoparticles in weakly acidic solution even though it did not significantly increase the rate of silica polycondensation. These results represent the first investigation regarding the kinetic aspect of utilizing chitosan in the biomimetic synthesis of silica. Because polypeptides, aminoglycans, and glycoproteins are widely present in various natural organisms, we suspect that these biopolymers may also play a similar role in accelerating the nanoparticle aggregation or silica biomaterial synthesis during the biosilicification process. Biopolymers vary diversely in structures and conformations; they not only serve as the construction templates in nature but also provide useful tools for humans to manipulate the structures of novel nanomaterials.

Acknowledgment. This research is partially supported by the National Science Council, Taiwan, Republic of China (Grants NSC 93-2120-M-019-001 and NSC 93-2313-B-019-023), and the National Taiwan Ocean University (Grant NTOU-AF94-04-03-01-01). The authors greatly appreciate the assistance of Dr. J. S. Hwang on the AFM measurement. We greatly thank Professor R. H. Chen (National Taiwan Ocean University) for the light-scattering particle-size determination, and Professor Ying-Chih Lin and Miss Ching-Wei Lu (Instrumentation Center, National Taiwan University) for their assistance in the elemental analysis.

Supporting Information Available: The integral method of analysis of kinetic data during silica formation; characterization of silica−chitosan nanoparticles using FTIR; changes in the turbidity of the silica−silicate solution; AFM image of silica−chitosan nanoparticles after reacting for 4 h; X-ray diffraction of silica−chitosan nanoparticles (pdf). This material is available free of charge via the Internet at http://pubs.acs.org.

CM052161D